JOURNAL OF PROPULSION AND POWER
Vol. 28, No. 2, March–April 2012

High-Speed and High-Reynolds-Number Jet Control Using Localized Arc Filament Plasma Actuators

M. Samimy,* M. Kearney-Fischer,† J.-H. Kim,‡ and A. Sinha§
Ohio State University Columbus, Ohio 43235-7531

DOI: 10.2514/1.B34272

A class of plasma actuators called localized arc filament plasma actuators for high-speed and high-Reynolds-number flow and acoustic control has been developed at the Gas Dynamics and Turbulence Laboratory. Over the past several years, these high-bandwidth (0 to 200 kHz) and individually controlled actuators have been used successfully to excite the jet shear layer, jet column, and azimuthal instabilities in high subsonic and supersonic jets. The focus of this paper is to provide detailed information and sample results highlighting the capabilities and potential of the actuators and the control technique for mixing enhancement, noise mitigation, and flow and acoustic diagnostics. The jet, using three different nozzles, is operated over a large range of jet Mach numbers (0.9 to 1.65), stagnation temperature ratios (up to 2.5), and Reynolds numbers (0.2×10^6 to 1.65×10^6). Over this space of operating conditions, the jet is found to respond to control with a large range of forcing Strouhal numbers and azimuthal modes. The results reveal that the jet flowfield and acoustic far field can be dramatically altered, providing a powerful control tool in these practical high-speed and high-Reynolds-number jets.

I. Introduction

FLUID flows are ubiquitous in countless systems and devices as well as in nature. Over the past several decades, tremendous research effort has gone into the development and implementation of flow control techniques to improve the beneficial effects and/or to reduce the detrimental effects of flows. The nature of the flow control technique used in an application depends on many factors, such as flow type, speed, Reynolds number, cost versus benefit assessment, etc. Numerous flow control techniques have been developed and used over the years in response to this broad range of requirements, making a complete categorization quite challenging. Two broad categories of passive and active controls have been used in the literature. Passive control almost always involves geometrical modifications, such as vortex generators on a wing of an aircraft for flow separation delay or chevrons on the exhaust nozzle of an aircraft for noise mitigation. Passive control devices are always on, regardless of whether they are needed or the performance penalty that they may incur. Active flow control, on the other hand, involves energy or momentum addition to the flow or the system in a regulated manner, and therefore can be turned on or off as needed. Active control is more desirable over passive control, as it can be turned off when it is not needed to save energy as well as to avert its potential detrimental effects, if it can be implemented effectively. Since active control is the subject of this paper, it will be further discussed.

Presented as Paper 2011-0977 at the 49th Aerospace Science Meeting, Orlando, FL, 4–7 January 2011; received 3 March 2011; revision received 26 May 2011; accepted for publication 4 September 2011.

*John B. Nordholt Professor of Mechanical and Aerospace Engineering, Gas Dynamics and Turbulence Laboratory, Aeronautical and Astronautical Research Laboratories, Department of Mechanical and Aerospace Engineering, 2300 West Case Road; samimy.1@osu.edu. Fellow AIAA.

†Ph.D. Student, Gas Dynamics and Turbulence Laboratory, Aeronautical and Astronautical Research Laboratories, Department of Mechanical and Aerospace Engineering, 2300 West Case Road. Student Member AIAA.

‡Research Associate, Gas Dynamics and Turbulence Laboratory, Aeronautical and Astronautical Research Laboratories, Department of Mechanical and Aerospace Engineering, 2300 West Case Road. Member AIAA.

§Ph.D. Student, Gas Dynamics and Turbulence Laboratory, Aeronautical and Astronautical Research Laboratories, Department of Mechanical and Aerospace Engineering, 2300 West Case Road; currently Postdoctoral Researcher, California Institute of Technology. Student Member AIAA.

II. Background

A. Active Flow Control

Active flow control is divided into two general categories: open loop and closed loop, or feedback. In the former, the actuation is dictated by an operator based on prior knowledge of the flow. In the latter, there is at least one sensor in the flow to measure the effect of actuation as well as the changes in the flow conditions. At each instant, the measured information is used by either a flow model [1] or an optimization algorithm based on minimal prior knowledge of the flow [2] to prescribe the actuation parameters for the next instant. The focus of this paper is on open-loop control, but our jet feedback control effort using localized arc filament plasma actuators (LAFPAs) will be briefly discussed.

Active control can also be classified based on the mechanism of its coupling with the flow. The first category can be called momentum injection or body force production. In this category, for example, the low momentum near-surface flow is energized, as in flow separation control over an airfoil by fluid injection (e.g., [3]), or a body force is generated, as by dielectric barrier discharge (DBD) plasma actuators (e.g., [4]). In this momentum injection category, additional flow structures (often streamwise vortices) are used, as for noise mitigation using fluidic chevrons [5]. The second category involves excitation of known flow instabilities by providing perturbations with frequency and mode within the ranges for which the flow is unstable. The seeded perturbations are amplified by the flow instabilities and develop into flow structures of the desired characteristics [6]. Indications are that momentum injection and body force-type controls have practical limitations in high-speed and high-Reynolds-number flows due to excessive energy input requirements, whereas such limitations do not seem to exist in control based on instability excitation. A good case in point is the use of traditional DBD actuators [7] with limitations in high-Reynolds-number flow separation control versus nanosecond pulse-driven DBD actuators with seemingly no such limitations [8,9].

B. Jet Instabilities and Receptivity

Jet instabilities will be briefly reviewed here; for a detailed discussion, see (e.g., [6,10]). An axisymmetric jet has two length scales: the initial jet column diameter or the nozzle exit diameter (D), and the initial shear layer or the nozzle exit boundary-layer momentum thickness (θ). Detailed instability analyses (e.g., [11]) and experimental results (e.g., [12]) show that the shear layer is receptive to perturbations over a large range of forcing frequencies (f_F). The forcing Strouhal number ($\mathrm{St}_{\theta F} = f_F \theta / U_j$) ranges from 0.01 to 0.02, where U_j is the jet exit velocity. This frequency range is approximately 40 to 80 kHz in our Mach 1.3 jet with $\theta \approx 0.1$ mm. Maximum growth rate is achieved when the shear layer is forced at $\mathrm{St}_{\theta F} \approx 0.017$, and maximum growth occurs in a naturally growing shear layer at $\mathrm{St}_\theta \approx 0.012$ (note that the F is omitted from the subscript since the variable does not refer to a forced quantity). The jet column instability frequency scales with D, so that the Strouhal number for the column mode instability is $\mathrm{St}_{DF} = f_F D / U_j$. The jet column is unstable for perturbations over the range $\mathrm{St}_{DF} \approx 0.2$ to 0.6, but the maximum growth of perturbations is obtained when the jet is forced at $\mathrm{St}_{DF} \approx 0.3$ (e.g., [13]). For later reference, the Reynolds numbers for free jets are defined as $Re_D = DU_j/\nu$, where ν is the kinematic viscosity at the nozzle exit.

In addition to the initial shear layer and the jet column mode instabilities, axisymmetric jets are also susceptive to azimuthal mode instability. The primary parameter affecting the development of azimuthal modes is D/θ (e.g., [14,15]). The linear stability analysis of Cohen and Wygnanski [15] showed that, for a very thin boundary layer (or very large D/θ), many azimuthal modes are unstable in the initial shear layer region. As will be discussed further, $D/\theta \approx 250$ in the work reported here, and the jet is indeed receptive to many forcing azimuthal modes.

The excitation of instabilities in a given flow strongly depends on where the perturbations are introduced, among several other factors. There is a significant body of literature on the receptivity of free shear layers and jets to external perturbations (e.g., [16]). It is generally agreed that 1) the receptivity is maximum where the shear layer is initiated, namely, at the nozzle exit or splitter plate edge; 2) the receptivity is in general better when the perturbations are introduced upstream rather than downstream of the nozzle exit or splitter plate edge; and 3) jets and free shear layers with laminar initial shear layers are more receptive than those with turbulent initial shear layers. As will be detailed later, the actuators in the current work are located just upstream of the nozzle exit, as close to the maximal receptivity location as physically possible.

C. Objectives of Jet Control

The linear stability analysis reported over three decades ago clearly showed that the jet is like a band-limited amplifier (e.g., [11]). This finding, along with the visual discovery of large-scale structures in relatively high-Reynolds-number jets and free shear layers [13,17], spurred tremendous activity in various aspects of shear layer and jet control over a span of almost 25 years. The objectives of the activities could be loosely divided into noise amplification, mixing enhancement, noise mitigation, and flow diagnostics. These topics will be briefly discussed in the next few paragraphs.

Aircraft noise comprises many components, including noise from fan, compressor, combustor, turbine, jet, and aerodynamic surfaces. Jet noise is the dominant component in takeoff and a major component in landing. Each component possesses distinct characteristics that are used to identify it in the acoustic signature of the aircraft. The individual components have been studied in laboratories, and corresponding models have been developed and tested over several decades. However, when these models are used to calculate the total noise from several components, including the jet noise, they often significantly underpredict the broadband jet noise from an actual jet engine [18–21]]. Understanding of this perplexing issue has challenged researchers for several decades. It was suspected that other noise components, especially those with pure tone components, from the fan, turbine, or combustor were interacting with and exciting the jet, thereby elevating the broadband noise in actual jet engines [22,23]. To test this hypothesis, researchers introduced pure tone excitation into laboratory jets and studied their broadband noise amplification characteristics. More detailed information and many references on this topic, as well as on the related research on bulk-mixing enhancement, can be found in Samimy et al.'s [10].

Jet noise mitigation using active control was attempted in the 1970s and 1980s. However, due to limitations in the excitation amplitude and frequency of the acoustic drivers used for actuation, the investigations focused exclusively on either low-Reynolds-number (less than 10^5) jets or moderate-Reynolds-number jets but with low frequency excitation enabling only jet column excitation. In addition, it is not easy to excite azimuthal modes using acoustic drivers, especially in high-speed flows. The results in the literature consistently show broadband turbulence amplification as well as far-field noise amplification with pure tone forcing at a Strouhal number around the jet column mode and up to about 1 ($\mathrm{St}_{DF} = 0.2$ to 1). The broadband amplification in turbulence and far-field noise was obtained regardless of whether the nozzle exit boundary layer was laminar or turbulent [18,23–26]. In works using much higher forcing Strouhal numbers ($\mathrm{St}_{DF} > 1.5$), the reported results heavily depended on the state of the boundary layer. In low-Reynolds-number jets with laminar nozzle exit boundary-layer, broadband turbulence suppression [12] as well as far-field noise suppression [27,28] were observed at forcing Strouhal numbers within the jet initial shear layer instability range ($\mathrm{St}_{\theta F} \approx 0.012$ to 0.017). When the boundary layer at the nozzle exit was turbulent, Zaman and Hussain [12] observed no effect on broadband turbulence levels, but Moore [18] and Jubelin [29] observed a suppression of 1 to 2 dB in the far-field noise. The broadband suppression or amplification seemed to be almost uniform over the entire frequency range and over a large range of polar angles with respect to the jet axis.

The use of an active jet control as a flow and noise diagnostic aid has paralleled the study of noise amplification/mitigation described. The three interconnected diagnostic objectives of low-amplitude tone excitation have been 1) raising the large-scale coherent structures above the background levels, 2) exciting shear layer instabilities, and/or 3) providing a phase reference for measurements. In the seminal work of Crow and Champagne [13] that established the presence of large-scale structures in relatively high-Reynolds-number jets ($Re_D \approx 10^5$), the well-defined time base provided by periodic excitation was used to analyze the data from hot-wire anemometry and schlieren imaging. Subsequently, many investigators sought to understand the development, evolution, and interaction of these structures, both axisymmetric and helical, using phase-averaged imaging and measurements (e.g., [12,27,30–35]). The implication of these discoveries in forced jets for the structure of unforced jets has been debated all along. Crighton [23] and Hussain [36] reviewed various related coherent vortex eduction techniques and discussed some of the relevant issues in the interpretation of such results.

The study of jets with seeded perturbations also has a natural link with instability theory, which predicts the evolution of such perturbations. Several researchers sought to compare and validate experimental data with theoretical predictions using time-averaged velocity and pressure statistics in the shear layer (e.g., [15,37–39]). The regularization of the jet structure obtained with low-amplitude excitation has also been of interest in the study of the large-scale structures as noise sources (e.g., [40,41]). Owing to actuator limitations, most of these efforts were limited to low-Reynolds-number jets and the axisymmetric forcing mode. One of the few investigations that covered high-speed and high-Reynolds-number jets and explored some of the above ideas, including nonaxisymmetric forcing, was the extensive study performed by the Lockheed Georgia group in the 1980s (e.g., [26,42], and references therein).

D. Actuator Requirements

Acoustic drivers were used for the majority of shear layer and jet active control in the past with the upper limit of $Re_D \approx 10^5$ for most of the work. In a laboratory-scale experimental facility, as the speed and the Reynolds number of the jet increase, so do the background noise, the instability frequencies, and the flow momentum. Therefore, actuators must provide excitation signals of much higher amplitudes and frequencies: two diametrically opposed requirements. As a result, there is practically no work on the active control of high-speed and high-Reynolds-number jets, with only a few exceptions. For example, Kibens et al. [43] used high-amplitude pulsed injection to excite the exhaust from a full-scale jet engine at a mixed azimuthal or flapping mode ($m = \pm 1$) around the jet column Strouhal number. They used two actuators, operating 180° out of phase and each covering a quarter of the exhaust jet perimeter. This resulted in significantly increased mixing and far-field noise radiation. Obviously, the increased scale, and thus the reduced frequency (~135 Hz), was a key factor in the implementation of actuation in this work. Moore [18], Jubelin [29], Ahuja et al. [44], Lu [20], and Lepicovsky and Brown [45] used acoustic forcing (either channeled the acoustic signal to multiple locations at the proximity of the exit of the jet or used it in the jet settling chamber) to force a high subsonic jet around its column mode. Apart from acoustic drivers, researchers have reported limited use of glow discharge in low-Reynolds-number jets [30,40], miniature piezoelectric zero-net-mass-flux devices in a high subsonic jet [46], and arc discharge and laser energy deposition in supersonic jets [35].

We have recently developed a class of plasma actuators, called LAFPAs, that can provide excitation signals of high amplitude and high bandwidth for high-speed and high-Reynolds-number flow control [6,47]. The actuator frequency, phase, and duty cycle can be controlled independently. Therefore, several of these actuators can be used to excite jet column modes, shear layer instability modes, and their various azimuthal modes. In the following sections, we will provide a brief background on LAFPAs.

III. Localized Arc Filament Plasma Actuators and Control Mechanisms

A LAFPA consists of a pair of electrodes: one attached to ground and the other to a power supply capable of generating high voltage on the order of several kilovolts. An electrically insulating and temperature-resistant annular extension is mounted on the nozzle exit. The eight LAFPAs used in the current work are distributed uniformly around the nozzle extension perimeter approximately 1 mm upstream of the exit (Fig. 1). The distance between the two electrodes in a LAFPA is normally 3 to 4 mm, center to center. When the voltage across a pair of electrodes is ramped up to the breakdown voltage (which is several kilovolts and depends on the distance between the electrodes, the air flow properties, and the frequency of operation), the air between the electrodes breaks down and an electric arc is generated. Right after the breakdown, the voltage across the electrodes drops to a few 100 volts and remains at that level until the voltage source is disconnected. The frequency and the duty cycle (the percentage of the time that the electrodes remain connected to the power supply relative to the forcing period) of each actuator are controlled independently by a dedicated computer. The frequency can be changed from near 0 to 200 kHz. With the eight actuators,

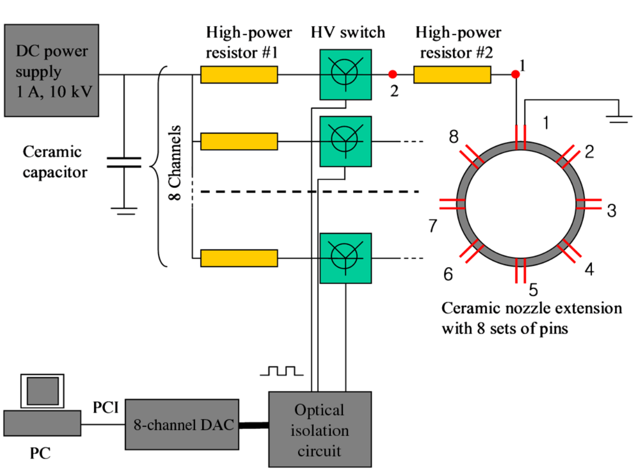

Fig. 1 Schematic of the LAFPA circuit with the eight LAFPAs distributed azimuthally just upstream of the nozzle extension exit (HV denotes high voltage, and DAC denotes digital-to-analog card).

simple azimuthal modes (m) from 0 to 3 and mixed modes ± 1, ± 2, and ± 4 can be excited by controlling the firing order of the actuators, as briefly explained below. The concept and earlier development of LAFPAs can be found in work by Samimy et al. [48], and the latest development and characterizations are given by Utkin et al. [47] and Samimy et al. [6].

In controlling a jet using acoustic drivers, the input signal is $A = A_0 \sin(2\pi f_F t - m\psi)$ for simple azimuthal modes, where A_0 is the amplitude, t is time, and ψ is the azimuthal location of the actuator. In the plasma actuator, the input signal is a rectangular on/off pulse. It is relatively simple to visualize the input signal. The azimuthal angle between two adjacent actuators is $\pi/4$, as shown in Fig. 1. The azimuthal angle between two actuators fired successively is determined by $\phi = 2m\pi/N$, where N is the number of actuators used (eight in the current work). Therefore, for example, $\phi = 0$ for $m = 0$ mode and all the actuators are operated in phase (at the same time), and $\phi = 3\pi/4$ for $m = 3$ mode and the order of actuators operation is 1, 4, 7, 2, 5, 8, 3, 6. For the mixed mode $m = \pm 1$, the top three actuators (8, 1, 2) and bottom three actuators (4, 5, 6) are operated 180° out of phase, and actuators 3 and 7 are inactive.

The duty cycle of the actuators can be varied from approximately 3 to 50%. At the lower end, there may not be sufficient time for breakdown and the actuators could misfire. At the higher end, the resistors in the circuit, used to limit the current, heat up too much and the cooling capacity of the system is not sufficient to handle the heat load. The duty cycle has a significant influence on the effectiveness of control. The optimum duty cycle is found to be the minimum duty cycle just sufficient to produce complete air breakdown between the electrodes [49].

In our earlier work, the electrodes were flush mounted with the inner surface of the nozzle. However, the plasma was noticeably stretched by the momentum of the high-speed flow and eventually swept downstream, causing reduction in the effectiveness of the actuation [48]. Therefore, we currently use a circular groove of 1 mm width and 0.5 mm depth, located approximately 1 mm upstream of the nozzle exit, to shelter the plasma. The tips of the electrodes are housed within this groove. In the most recent work, a new nozzle extension was designed, which relocated the electrodes to the nozzle extension face and eliminated the ring groove. The results showed that the effect of the ring groove is secondary and relatively small [49]. Kleinman et al. [50] used direct numerical simulations in a recent work to investigate the effect of the groove on the actuation process in a flow that matches the experimental flow conditions for a Mach 1.3 jet. However, due to the current computational resource limitations, the flow and cavity geometry was restricted to two dimensions, even though the flow within the cavity was clearly three-dimensional. Because of this limitation, the simulation results significantly overpredicted the effect of the cavity.

The short duration and harsh high-temperature environment of plasma create a major challenge for any accurate measurements of perturbations imparted to the flow by the actuators. We have used nitrogen emission spectroscopy to measure the average temperature of the plasma, which depends on the frequency and duty cycle of the operation. The temperature, averaged over the spatial extent of the plasma (approximately 1 mm wide and 3 to 4 mm long) and, over several pulses, varies from a few 100 to about 1200°C [51]. For example, the measured average temperature with 5 kHz forcing and 15 μs pulse duration (7.5% duty cycle) is ~1000 °C.

The jet is known to be receptive to thermal, aerodynamic, and acoustic perturbations [18]. With LAFPAs, the initial perturbation is thermal (i.e., localized joule heating by the air breakdown). However, the flow is compressible and each breakdown causes rapid microsecond timescale localized heating that generates a compression wave [10]. Our earlier unsteady quasi-one-dimensional model of the arc filament showed that the rapid localized heating generated compression waves that were steepened in a short period (~10 μs) and in a short distance (~3 mm) to become a stronger compression wave [47], in general agreement with the experimental results. It is not possible to discern whether it is the thermal perturbation, the pressure perturbation, or a combination of the two that is coupled to the flow. However, thermal perturbation seems to be more plausible, as it was successfully used in recent simulations [52,53], which will be discussed. Earlier results showed that the actuators could generate streamwise vorticity and vortical/aerodynamic perturbations, the strength of which depends on the distance between the electrodes [48]. However, with 3 or 4 mm distance between the electrodes in the current work, and potentially nonuniform plasma between the electrodes, the generated streamwise vorticity is expected to be quite weak.

A recent numerical simulation work involves large eddy simulation and uses eight actuators and flow parameters similar to those in the current Mach 1.3 jet experiment, and it simulates the effects of actuation as a periodic surface heating [52,53]. The response of the jet to the actuation and the ensuing structures are very similar to those in the experiments. Another large eddy simulation effort involves details of nozzle geometry and actuators arrangement [54]. It models the plasma as a simple time-varying and spatially distributed internal energy source, similar to the model used by Utkin et al. [47]. The preliminary results of this work show generation of compression waves by the actuation, similar to those observed experimentally.

IV. Experimental Facility and Techniques

A brief description of the experimental facility and techniques used at the Gas Dynamics and Turbulence Laboratory within the Aeronautical and Astronautical Research Laboratories (AARL) at the Ohio State University is given in this section. The jet is created using compressed air and contoured converging and converging–diverging nozzles of exit diameter $D = 2.54$ cm (1 in.), designed using the method of characteristics. The air is compressed by three five-stage reciprocating compressors: filtered, dried, and stored in two cylindrical tanks with a volume of 43 m^3 and pressure up to 16 MPa. The compressed air is supplied to the stagnation chamber of the jet facility, discharged horizontally through the nozzle into an anechoic chamber, and then discharged through an exhaust system to the outdoors (Fig. 2). Recently, the jet facility was remodeled and a new anechoic chamber was built. The new jet facility is capable of using 1 to 2 in. jets and up to 16 actuators. This enables the usage of azimuthal modes up to seven to further evaluate the benefits of higher azimuthal modes for noise mitigation. The footprint of the anechoic chamber is increased by a factor of 2.4, enabling far-field acoustic measurements from a 25 to 140° polar angle with respect to the downstream jet axis for assessing the effect of control on shock noise in supersonic jets.

Far-field sound pressure is measured using a linear array of $\frac{1}{4}$ in. B&K 4939 microphones covering 25 to 90° polar angles with respect to the jet axis. The far-field acoustic results are scaled to a distance of 80 jet diameters. The acoustic signal from each microphone is bandpass filtered from 20 to 100 kHz, amplified by B&K Nexus 2690 conditioning amplifiers and acquired using National Instruments A/D boards and LabVIEW software. The microphones are calibrated using a 114 dB, 1 kHz pure sinusoidal tone. The frequency response of the microphones is flat up to 80 kHz with the microphone grid cover removed. Blocks of data were collected at 200 kHz with 8192 data points per block, producing a spectral resolution of 24.4 Hz. The sound pressure level spectrum is obtained by averaging 100 blocks of data.

A LaVision particle image velocimetry (PIV) system with a 2048×2048 pixel resolution camera is used for two-component (streamwise and radial) velocity measurements on a vertical plane passing through the jet centerline. A Spectra Physics Model SP-400 dual-head Nd:YAG laser is used as the light source. The cameras and laser are synchronized by a timing unit housed in a dual processor PC. The spatial resolution of the velocity vectors depends on the field of view and the number of pixels used. For most of the streamwise velocity field measurements, the spatial resolution is about 2.2 mm. The laser sheet thickness is less than 0.3 mm. The time separation between two consecutive PIV images ranges from 1.8 to 4 μs (depending on jet exit velocity) so the velocity field from a pair of PIV images is almost instantaneous. In initial processing, an interrogation window of 64×64 pixels is used. Then, the reduced data are used as a reference in final processing with an interrogation window of 32×32 pixels with 50% overlap to increase spatial resolution of the computed vector fields. PIV data are collected as 700 statistically random snapshots. Turbulence statistics are obtained using 700 image pairs; convergence of statistics is achieved with 600 to 650 image pairs. Phase-averaged flowfields are constructed by conditional averaging of the random data set computed as a postprocessing step. More information on this process can be found in [55,56].

The jet plume is seeded with liquid droplets atomized by a four-jet LaVision atomizer in unheated jets. For heated jets, aluminum oxide particulates suspended in ethanol are used [55]. A 38.1 cm duct, made of 1-mm-thick sheet metal, is placed around the jet to generate a very low-speed coflow (see Fig. 2). The coflow velocity is less than 3 m/s (less than 1% of the jet exit velocity). The coflow is generated by allowing a significant portion of the ambient air entrained into the jet to pass through the duct. The coflow is seeded by a Concept Model ViCount Compact 1300 fogger to avoid statistical bias in the measurements, as well as the computation of spurious velocity vectors in the entrained air that are not yet mixed with the jet. The average droplet sizes are about 0.7 and 0.25 μm for the jet flow and coflow, respectively. The solid particles have a mean diameter of 0.6 μm.

Schlieren images of the jet are collected using a Z-type schlieren system. The system uses a Palflash 501 high-intensity illumination flash unit with a flash duration of approximately 500 ns, which is short enough to create a quasi-frozen flowfield during imaging. Phase-locking the schlieren images to the actuator control signal allows for observation of details of flow and wave structures.

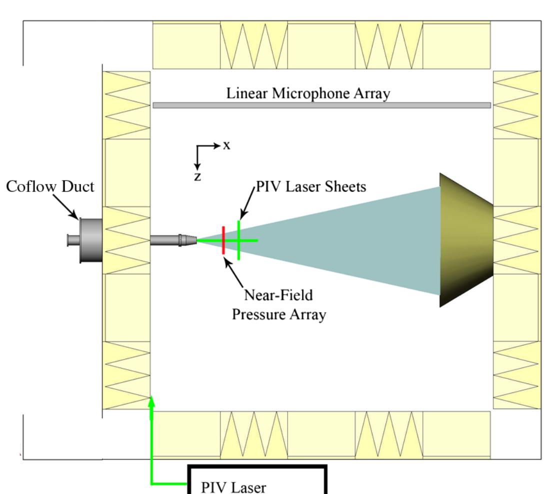

Fig. 2 Schematic of jet and anechoic chamber.

V. Experimental Results

Over the past several years, detailed experiments have been carried out to investigate the effects of LAFPAs on both the flowfield and far-field acoustics of unheated and heated Mach 0.9, 1.3, and 1.65 jets [6,55,57–62]. For the Mach 1.65 jet, two nozzles are used: a standard contoured nozzle designed using the method of characteristics, and a conical nozzle (both conical converging and diverging sections, with a sharp throat) typical of the variable area nozzles used in tactical aircraft. The ratio of the stagnation temperature of the jet to the room temperature (TTR) is varied from 1 to 2.5, and Re_D is varied from approximately 2×10^5 to 1.7×10^6. We have also carried out limited reduced-order model development and feedback control work using a Mach 0.9 jet [2,63]. Only some selected results are presented and discussed below.

A. Boundary Layer at the Nozzle Exit

It has been known that the state of the boundary layer at the nozzle exit plays a significant role in the response of the jet to excitation and

Table 1 Important jet parameters

M_j	TTR	M_a	$M_{c,\mathrm{th}}$	$M_{c,\mathrm{emp}}$	$Re_D \times 10^{-6}$
0.9	1.0	0.83	0.43	0.50	0.61
	1.5	1.02	0.47	0.61	0.36
	2.0	1.18	0.50	0.71	0.26
	2.5	1.32	0.53	0.79	0.20
1.3	1.0	1.12	0.60	0.84	1.07
	1.5	1.38	0.66	1.04	0.63
	2.0	1.59	0.71	1.19	0.44
	2.5	1.78	0.74	1.34	0.34
1.65	1.0	1.33	0.73	1.00	1.65
	1.5	1.63	0.81	1.22	0.96
	2.0	1.88	0.87	1.41	0.67
	2.5	2.1	0.92	1.56	0.51

in the initial development of structures in the shear layer of the jet. The 2.54 cm (1 in.) inner diameter axisymmetric nozzles with design Mach numbers of 0.9, 1.3, and 1.65 (except for the 1.65 conical nozzle) all have smooth and gradual converging and diverging sections. In addition, a 2.54 cm inner diameter nozzle extension with a length of 1.9 cm (0.75 in.), which is attached to the nozzle to house the actuators, provides relaxation to the boundary layer developed within the nozzle. With a high Reynolds number and the geometry as described, the boundary layer is expected to be turbulent. However, the boundary-layer thickness is estimated to be on the order of 1 mm, which makes it nearly impossible to make measurements at a sufficient number of points within the boundary layer to determine its characteristics.

We recently used a 3.8 cm (1.5 in.) converging nozzle attached to the current jet facility and a hot wire to make measurements within the initial shear layer of an unheated subsonic jet, approximately 2 mm downstream of the nozzle exit [55]. We limited the Mach number from 0.25 to 0.65 (Reynolds number approximately from 2×10^5 to 6×10^5) to avoid significant density variations and complications with hot-wire measurements and interpretations. When the nozzle extension was attached, all the normalized profiles for various Mach number and Reynolds number jets were collapsed into a single curve, thereby indicating turbulent flow over the range of Reynolds numbers tested. Note that 2×10^5 is the lowest Reynolds number (for Mach 0.9 and temperature ratio of 2.5) used in the actual jet experiments. On the other hand, without the nozzle extension for the boundary-layer relaxation, the profiles did not collapse, indicating either a laminar or transitional boundary layer. These results confirm that the boundary layer at the nozzle extension exit in the actual jet work is turbulent.

Fitting a hyperbolic tangent curve to the velocity profiles and employing a technique used by Bechert and Stahl [64], the boundary-layer and momentum thicknesses were determined to be ~1.2 and 0.1 mm at the higher end of the Reynolds numbers [55]. Therefore, the best guess at this time is that the boundary-layer and momentum thicknesses in the jet are on the order of 1 and 0.1 mm.

B. Effects of Control on the Flow Structures

The effects of excitation using LAFPAs on the jet flow structures have been explored over a wide range of jet Mach numbers and temperatures. Table 1 shows the important jet parameters for the cases discussed in this paper, including the jet Mach number (M_j), acoustic Mach number (M_a), theoretical convective Mach number ($M_{c,\mathrm{th}}$) [65], empirical convective Mach number ($M_{c,\mathrm{emp}}$) typically used in the literature (for which the convective velocity is approximated by $0.65U_j$ for $M_j = 0.9$ and $0.75U_j$ for $M_j = 1.3$ and 1.65) [66–68], stagnation temperature ratio (TTR), and Reynolds number based on the jet diameter (Re_D). There is a myriad of publications in the literature on the identification of structures in a flow [69–72]. The three methods that we have found quite useful with the two-component PIV data are the techniques based on the Galilean streamlines [72], swirling strength [71], and Q criterion [69]. Combining the first one with one of the other two provides even better visualization of the structures in the high-Reynolds-number flows of interest in the current work.

Figure 3 shows superimposed phase-averaged Galilean streamlines and normalized Q criterion for an excited Mach 0.9 jet with a Reynolds number of about 0.61×10^6. The excitation is around the jet column frequency ($\mathrm{St}_{DF} = 0.33$), and the two excited azimuthal modes are 1) axisymmetric mode ($m = 0$) and 2) flapping mode ($m = \pm 1$). For the Galilean streamlines, the coordinate system is convecting with the large-scale structures. If there are relatively coherent large-scale structures in the flow and, if the convective velocity in the flow remains relatively uniform, the structures are identified by streamlines spiraling around a core or by closed streamlines, as shown in Fig. 3. The convective velocity used in the calculation of the Galilean streamlines is computed from the data using spatial correlations of the Q-criterion fields. The spatial correlations produce the structure spacing λ, and the convective velocity is calculated using $U_c = \lambda f_F$. This procedure and the various convective Mach number used in the literature are explained in more detail in [73].

The Q-criterion [Eq. (1)] separates the antisymmetric (rate of rotation) $\mathbf{\Omega}$ and the symmetric (rate of strain) $\mathbf{S}$ components of the velocity gradient tensor; therefore, it identifies the core (positive Q) and the braid (negative Q) regions of the structures in the flow, as shown in Fig. 3. In Figs. 3–5, the core and braid regions are identified by different colors and by added black and white circles:

$$Q = \tfrac{1}{2}(\|\mathbf{\Omega}\|^2 - \|\mathbf{S}\|^2) \tag{1}$$

Note that the Q criterion shown in the figures is normalized by $(D/U_j)^2$. Coherent structures are identified with both azimuthal modes of excitation in the cases shown. These structures grow in size and strength up to about $3D$ to $4D$, followed by weakening and eventual disappearance, either due to their interaction and disintegration or by developing jitter, thus getting smeared out in the conditional-averaging process. The main difference between the two excited azimuthal mode cases is in the arrangement of the structures: symmetric with respect to the jet axis in the $m = 0$ and antisymmetric in the $m = \pm 1$ cases. These two very different structure identification techniques agree quite well in identifying the structures and marking their core and braid regions.

Excitation around the jet column frequency with $m = 1$ (not shown) generates large-scale structures similar to those shown in Fig. 3. However, with higher azimuthal modes of excitation, identification of the structures on a planar view becomes much more

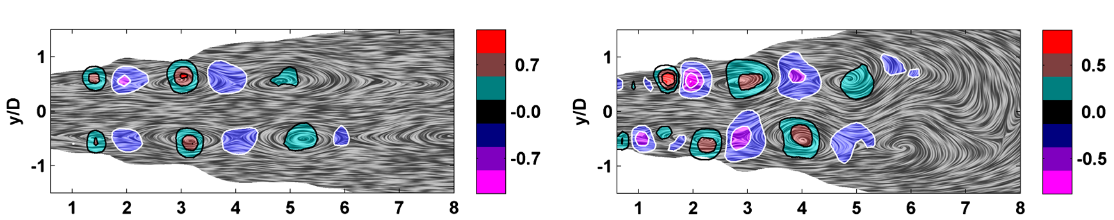

a) $m = 0$ b) $m = \pm 1$

Fig. 3 Superimposed phase-averaged normalized Q criterion and Galilean streamlines for Mach 0.9 unheated jet excited at $\mathrm{St}_{DF} = 0.33$ for a) axisymmetric azimuthal mode ($m = 0$) and b) first flapping mode ($m = \pm 1$).

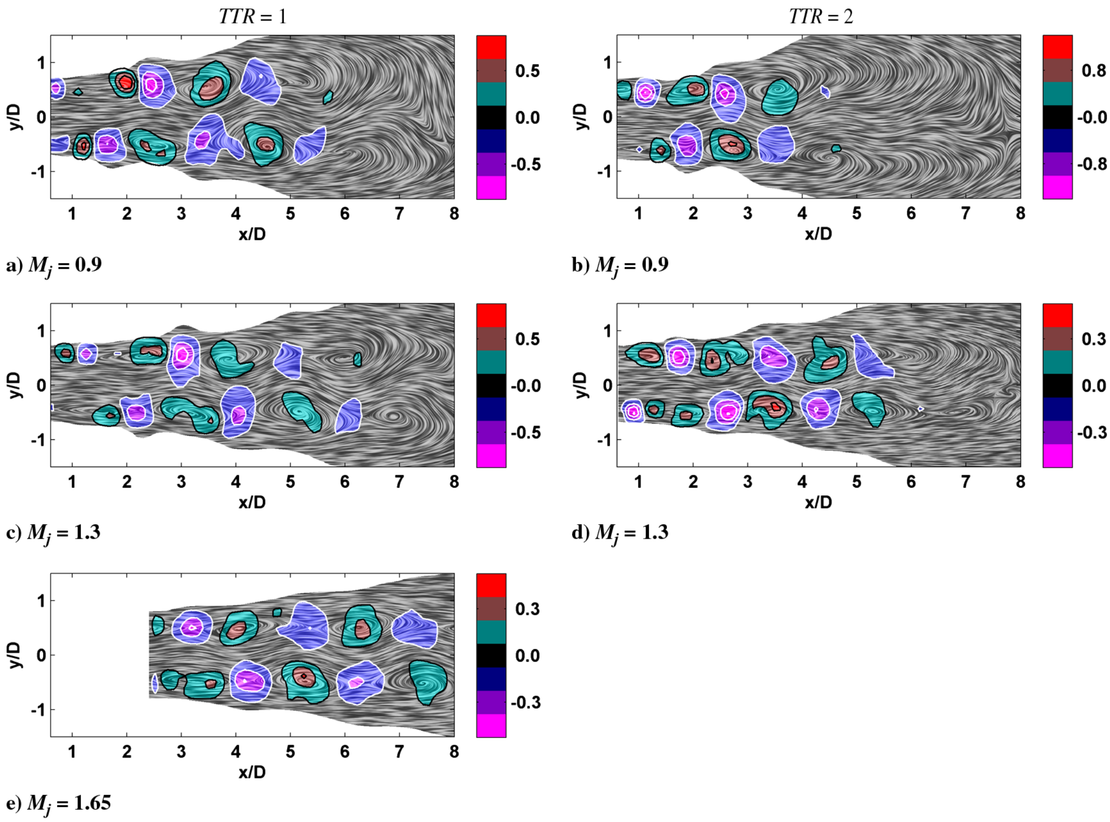

Fig. 4 Effects of excitation on flow structures at various jet Mach numbers and temperatures with forcing at $m = \pm 1$ and $\mathrm{St}_{DF} = 0.33$: unheated jet (Figs. 4a, 4c, and 4e) and heated jet (Figs. 4b and 4d) with stagnation temperature ratio TTR = 2.

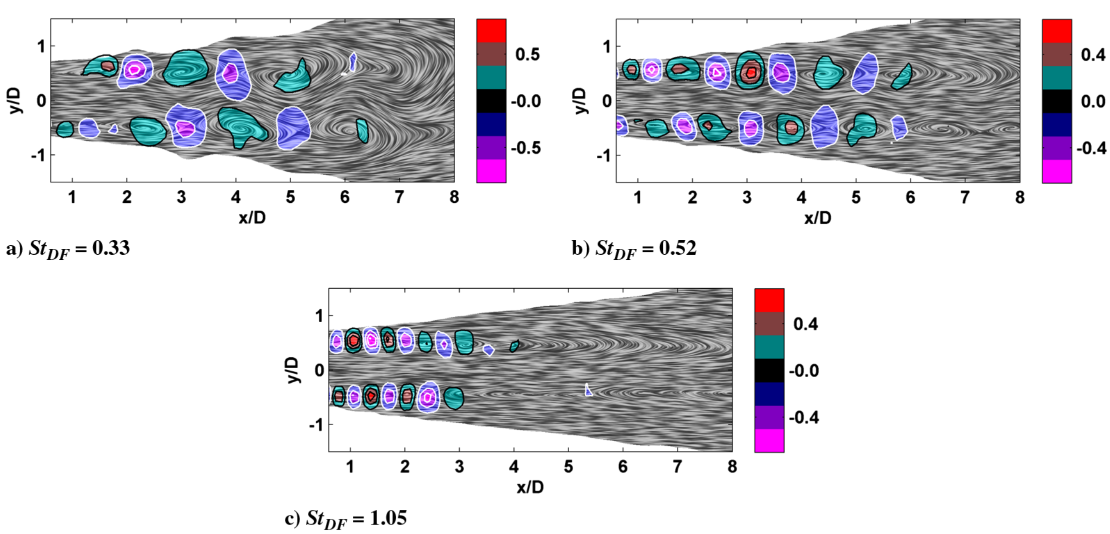

Fig. 5 Effects of forcing Strouhal number on flow structures: $M_j = 1.3$, TTR = 1, and $m = \pm 1$.

challenging. Recent numerical simulation results [52,53] show details of these structures in three dimensions and reveal intricacies of their evolution, interactions, and disintegration.

The effects of variations in the jet Mach number and temperature on the response of the jet to excitation are shown in Fig. 4. For all the cases shown, the forcing azimuthal mode and Strouhal number were kept at $m = \pm 1$ and $\mathrm{St}_{DF} = 0.33$. Surprisingly, even with the large changes in Reynolds number (0.26×10^6 to 1.65×10^6), convective Mach number ($M_{c,\mathrm{th}} = 0.43$ to 0.73 or $M_{c,\mathrm{emp}} = 0.50$ to 1.0), and acoustic Mach number (0.83 to 1.59), the response of the jet to the excitation seems to be quite similar and there are no major changes in the nature of the developed large-scale structures. The conclusion is similar in other excitation azimuthal modes and Strouhal numbers.

It is clear from the results presented in Figs. 3 and 4 that the jet responds in a similar fashion to excitation around the jet column Strouhal number regardless of the jet Mach number, temperature, or the excitation azimuthal mode. The effect of excitation Strouhal number at $m = \pm 1$ is shown in Fig. 5 for the unheated $M_j = 1.3$ jet. Increasing the St_{DF} from 0.33 to 0.52 reduces the size and spacing of the structures, as expected, but the structures remain coherent until $x/D \approx 7$, just downstream of the end of potential core, similar to those at the lower St_{DF}. At the higher St_{DF} of 1.05, the structures are still coherent and quite discernible, although much smaller, in the early part of the shear layer (up to $x/D \approx 4$), but they either disintegrate or develop significant jitter and get smeared out in the conditional-averaging process further downstream. This behavior of the structures is reflected also in the jet overall growth, in that the jet grows continuously even downstream of the end of the potential core when excited at lower St_{DF}, but it grows much faster up to $x/D \approx 4$ and saturates early at higher St_{DF} [10].

Only sample results of the excitation effects on the flow structures are shown in Figs. 3–5. Spatial correlation of PIV images were used to determine structure spacing in all the jets listed in Table 1 for various St_{DF} and m. Either the radial component of velocity [59] or Q criterion [61] were used to determine the structure spacing λ. The results shown in Fig. 6 more quantitatively illustrate the similar response of the jet to excitation regardless of the jet Mach number or temperature covering a large range of jet convective and acoustic Mach numbers. All the results collapse well on a single curve of equation

$$\frac{\lambda}{D} = \frac{0.51}{\mathrm{St}_{DF}} + 0.33 \qquad (2)$$

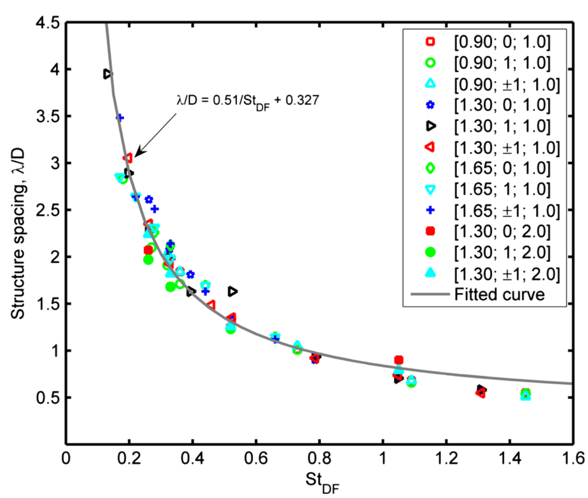

Fig. 6 Effects of St_{DF} on structure spacing for various jet Mach numbers, temperatures, and forcing azimuthal modes: the legend denotes [M_j; m; TTR].

C. Effect of Excitation on Far-Field Acoustics

The excitation can significantly alter not only the kinematics but also dynamics of large-scale flow structures. It is noteworthy that the actuation provides perturbations with selected frequency and mode, and the flow instabilities amplify them. These amplified perturbations roll up into large-scale structures. It has been known for quite some time in the literature that the dynamics of these large-scale structures are responsible for the peak noise in the shallow angles with respect to the downstream jet axis. Therefore, these actuators can be used as a tool to tailor the flow structures, and thus the far-field radiated noise. It should also be mentioned that we do not have direct control on small-scale flow structures, which are a byproduct of the interaction and disintegration of large-scale structures. The dynamics of these structures generate noise that primarily radiates to the sidelines (around 90°). Sample far-field acoustic results showing the effects of actuation on the far-field acoustics are presented and discussed in this section.

The two main effects of the control on the far-field acoustics are the appearance of the actuation tone and its harmonics, and the change in the broadband shape and level. Both of these strongly depend on polar angle of the observation as well as on the forcing Strouhal number and azimuthal mode. Figure 7 shows far-field spectra at two polar angles of 30 and 90° for a Mach 1.3 jet at two temperatures: unheated ($\mathrm{TTR} = 1.0$) and moderately heated ($\mathrm{TTR} = 2.0$) jets. The general trend of the effects of simple azimuthal modes ($m = 0, 1, 2, 3$) is that $m = 3$ provides maximum reduction in the peak noise around a 30° polar angle [as well as maximum reduction in the overall sound pressure level (OASPL)]. On the other hand, $m = 0$ provides maximum amplification around 90°, although at a lower St_{DF}. The four St_{DF} presented in Fig. 7 are chosen as follows: the two higher ones result in maximum noise reduction with $m = 3$ at 30° at the two temperature ratios indicated, and the two lower ones lead to maximum noise amplification with $m = 0$ at 90° at the two temperature ratios depicted. The following observations regarding the excitation tones can be made from the results shown in Fig. 7 and others not shown here:

1) The tone amplitude increases with the temperature.
2) The tone amplitude is much lower with $m = 3$ than $m = 0$.
3) The tone amplitude at 90° is much lower than that in 30°.

Preliminary results in a much larger facility showed much lower tone amplitude in comparison with the broadband noise amplitude [74]. More work on this issue is forthcoming. Regarding the broadband

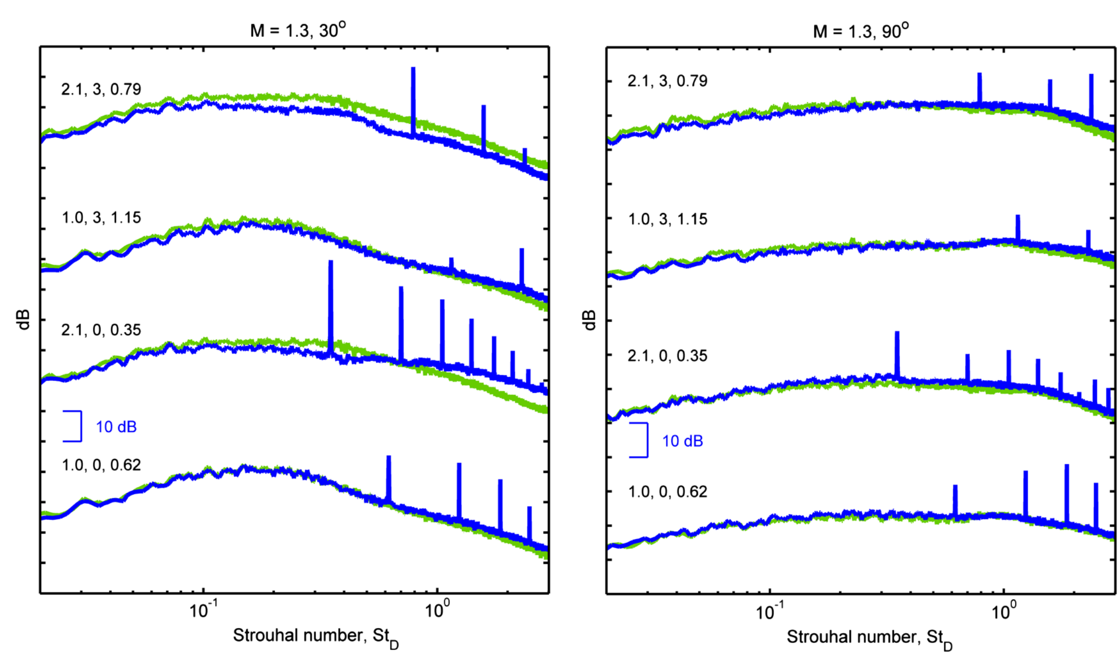

a) 30° polar angle **b) 90° polar angle**

Fig. 7 Far-field acoustic spectra for Mach 1.3 jet showing actuation tones and their harmonics: numbers next to the spectra are TTR, m, and St_{DF}. Forced spectra with forcing tones (dark) and corresponding unforced spectra with no tones (light) are overlaid.

noise amplitude, both noise reduction and amplification levels are increased with temperature. The effects of actuation on broadband noise are further discussed next.

Figure 8 shows the effect of St_{DF} on the $\Delta\mathrm{OASPL}(= \mathrm{OASPL}_{\mathrm{forced}} - \mathrm{OASPL}_{\mathrm{baseline}})$ for a Mach 1.3 jet at TTRs of 1.0 and 2.0, and for $m = 0$ and 3 over polar angles of 25 to 90°. In both temperature ratio cases, higher St_{DF} reduce broadband noise over all polar angles and lower St_{DF} increase it over all polar angles, except at $\mathrm{TTR} = 2$ at shallow polar angles, especially for $m = 3$ excitation. The effect of actuation is improved at the higher TTR, especially for $m = 3$ excitation at shallow angles and lower St_{DF}. While there is no Mach wave radiation in the unheated Mach 1.3 jet with $M_a = 1.12$ and $M_{c,\mathrm{th}} = 0.6$ ($M_{c,\mathrm{emp}} = 0.84$) (see Table 1), it is significant in the heated jet of $\mathrm{TTR} = 2$ with $M_a = 1.59$, and $M_{c,\mathrm{th}} = 0.71$ ($M_{c,\mathrm{emp}} = 1.19$) [73]. Mach wave radiation changes the nature of far-field noise, which includes a shift to higher polar angles of the peak noise.

Figure 9 is generated based on the results presented in Fig. 8 and other similar results, and it shows the effects of jet Mach number and temperature on the maximum noise reduction at a 30° polar angle with $m = 3$ excitation and on the maximum noise amplification at a 90° polar angle with $m = 0$ excitation. There is a clear temperature effect in the Mach 0.9 and 1.3 jets with significantly higher noise reduction at higher temperatures. However, the temperature does not have a clear effect on noise reduction in Mach 1.65. Raising Mach number and/or temperature moves the jet into the Mach wave radiation regime and changes the far-field noise characteristics. Mach wave radiation starts around $\mathrm{TTR} \approx 2.5$ in the Mach 0.9 jet, but it is relatively strong at higher TTR in the Mach 1.3 jet, and it is present even in the unheated Mach 1.65 jet [73]. In addition, the compressibility effect is relatively minor in a Mach 0.9 jet, even at $\mathrm{TTR} = 2.5$ ($M_{c,\mathrm{th}} = 0.53$, and $M_{c,\mathrm{emp}} = 0.79$), but it is quite strong in a Mach 1.3 jet ($M_{c,\mathrm{th}} = 0.71$, $M_{c,\mathrm{emp}} = 1.19$ at $\mathrm{TTR} = 2.0$) and in a Mach 1.65 jet ($M_{c,\mathrm{th}} = 0.73$, $M_{c,\mathrm{emp}} = 1.0$ at $\mathrm{TTR} = 1$). Currently, we do not have sufficient knowledge of the effects of Mach wave radiation or compressibility on the actuation authority.

Noise amplification at the sideline (Fig. 9) is not a desirable outcome but a byproduct of manipulation of large-scale structures by actuation. As was shown in Fig. 8, lower St_{DF} amplify noise over a large range of polar angles, especially at the sideline. There does not seem to be any trend in the temperature effect; however, there seems to be a Mach number effect with much higher amplification in lower Mach numbers. Since this is a byproduct of manipulation of large-scale structures by actuation, it is much harder to understand the effects of Mach wave radiation, compressibility, and other variables on noise amplification. Perturbation levels that are much higher than is needed could be one possible explanation of the much higher noise amplification in the Mach 0.9 jet. We do not have direct control on the perturbation level provided by the actuators; therefore, it is possible that eight actuators are excessive, but they are needed to force the higher azimuthal modes. Further investigation of this issue is forthcoming.

D. Near-Field Pressure Measurements for Feedback Control

A limited investigation has been performed on the pressure field in the irrotational region of the jet with the goal of incorporating its real-time sensing in a feedback control loop [2,10]. Earlier researchers had reported on the strong correlation between the velocity fluctuations associated with large-scale structures in the shear layer and the near-field pressure fluctuations [75–77]. Since the LAFPAs are shown to affect these large-scale structures, it was hypothesized that a real-time estimate of this effect may be sensed in the near-field pressure. Moreover, the axisymmetric mode of the near-field pressure has also been found to be strongly correlated with the intensity of the mixing noise radiated to the far field [78–80]. With this in mind, an azimuthal array of pressure sensors was developed and implemented in a simplistic feedback loop to determine the

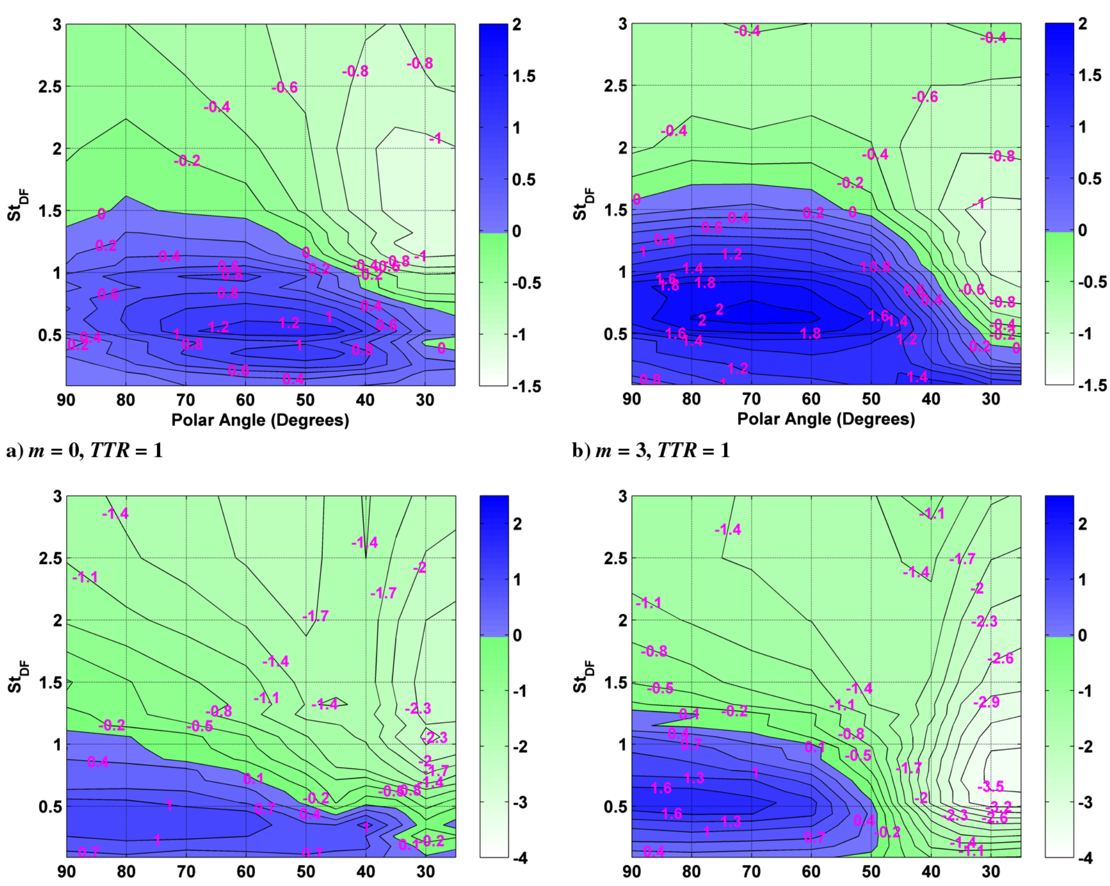

a) *m* = 0, *TTR* = 1
b) *m* = 3, *TTR* = 1
c) *m* = 0, *TTR* = 2
d) *m* = 3, *TTR* = 2

Fig. 8 Effects of St_{DF} on $\Delta\mathrm{OASPL}$ in the Mach 1.3 jet at $m = 0$ and 3 and $\mathrm{TTR} = 1$ and 2.

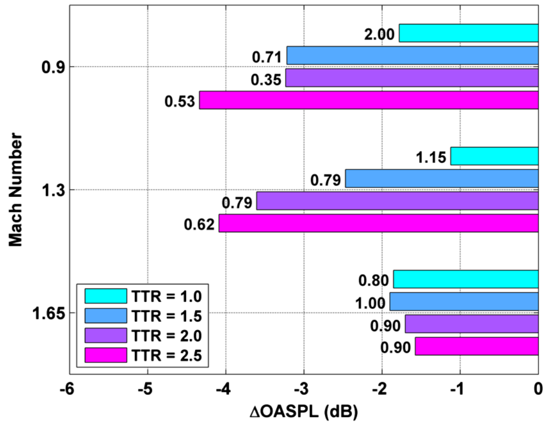

a) m = 3, 30º polar angle

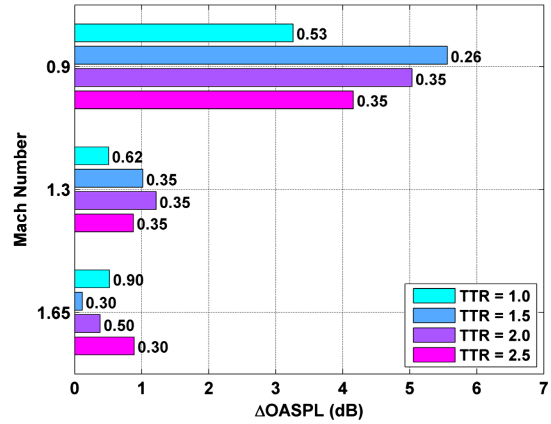

b) m = 0, 90º polar angle

Fig. 9 Maximum noise reduction and amplification at several temperature ratios: a) maximum far-field acoustic reduction at 30° polar angle with $m = 3$ excitation, and b) maximum noise amplification at 90° polar angle with $m = 0$ excitation at several jet Mach numbers and temperatures. St_{DF} are shown.

forcing parameters in real time that either 1) minimized fluctuations in the axisymmetric mode of pressure, or 2) maximized fluctuations in the sum of the axisymmetric and first helical modes [2]. Achievement of the first goal was indeed found to correspond to the forcing parameters converging upon the optimal values found in open-loop parameter sweeps, as reported in Figs. 8 and 9. The spectrum of the far-field pressure during steady-state operation of the controller also indicated this convergence. Imposition of the second objective was found to drive the forcing frequency to the jet column mode, which is optimal for bulk-mixing enhancement.

The simplistic feedback controller described above suffers from a slow rate of response compared with the timescales of the flow. To obtain faster controllability, one needs to develop a reduced-order model of the velocity field, along with a dynamic estimator and sophisticated control algorithms. This work is ongoing, and progress in this direction has been reported in [63,81].

E. Control Employed as a Tool for Flow and Noise Diagnostics

The results to date have shown that LAFPAs have the ability to manipulate jets over a wide range of Mach numbers and temperatures. However, the existing body of research with LAFPAs has been focused on specific applications for such manipulation (i.e., demonstrating the capabilities for mixing enhancement or noise control). While LAFPAs show great promise for these specific applications, the utility of LAFPAs as a diagnostic tool should not be overlooked.

The uses for LAFPAs as a diagnostic tool stem from two related effects: 1) the creation of a well-defined spatiotemporal origin for large-scale structures, and 2) the regularization of large-scale structure development. It should be obvious that these characteristics are similar to those provided by other active control techniques (e.g., acoustic drivers) that have been used in the past to great effect in the study of low-Reynolds-number jets. The distinguishing characteristic of LAFPAs is their effectiveness at high-Reynolds-number ($Re_D \approx 10^6$ or higher) unheated or heated jets, and high-bandwidth ($f \approx 100$ kHz) regimes where none of the other active control techniques have been effective. The turbulence in this high-Reynolds-number regime complicates analysis of the dynamic governing processes like noise production and vortex development/interaction. In short, LAFPAs can potentially do for the understanding of these high-Reynolds-number jets what acoustic drivers did for the understanding of lower Reynolds number flows by providing control authority in this regime.

LAFPAs produce perturbations that grow and give rise to structures when the frequency and mode of actuation fall within the range of instabilities in the flow. Depending on the firing parameters, the structures from individual LAFPAs may or may not merge into a cohesive structure (such as a ring vortex or helix). From the perspective of using LAFPAs as a diagnostic tool, the most important aspect of this forcing mechanism is that the time and location of perturbations that give rise to individual structures are quite narrowly defined. While the positional uncertainty of this origin is on the order of the electrode spacing (∼1 mm), the results to date indicate that the temporal uncertainty is quite low (∼20 ns). The high degree of temporal localization is based on the conclusion that the voltage breakdown process (which takes about 10–20 ns) is responsible for the control authority of LAFPAs. In contrast, determining the temporal origin for a structure produced by pure tone acoustic excitation to subperiod accuracy is quite difficult due to the smooth nature of a sinusoidal signal.

The high degree of localization in the spatiotemporal position of the perturbation opens areas of study that would be otherwise inaccessible. Pure tone excitation gave researchers the ability to localize events in terms of phase angle. LAFPAs, however, can provide a complete time history. Stability analysis shows that, under the appropriate conditions, a perturbation will grow and roll up into a structure, but the very beginnings of this roll-up process are impossible to observe unless one knows exactly where and when to look. However, by creating a well-defined spatiotemporal origin, LAFPAs provide a means of examining the growth and evolution of structures with a high degree of fidelity, limited by the other diagnostic tools being used in conjunction with LAFPAs. With the appropriate experimental equipment (or simulation parameters), the life of a single structure can be examined from beginning to end. This experimental capability, as might be expected, can also be used to perform analyses similar to those done with other flow control techniques (phase-locking, conditional averaging, etc.). For example, conditional averaging was employed in the calculation of Q criterion and Galilean streamlines shown in Figs. 3–5.

Another consequence of active control is the regularization of certain flow characteristics. The artificial perturbations have repeatable parameters that result in large-scale structures with more repeatable characteristics. As is seen in other control techniques, the large-scale structure growth rates, convective velocities, rotational energies, etc., are all regularized by forcing. This offers obvious benefits in the form of potential for examining these quantities in jets at different operating conditions with enhanced repeatability. This consequence of forcing also has implications for acoustics studies. As reported by Kastner et al. [60], LAFPA forcing has the effect of concentrating certain types of noise events into a smaller spatial region around the end of the jet potential core. With noise production events confined to a smaller domain, other diagnostic tools can be focused onto a smaller region, increasing the ability to examine the dynamics surrounding jet noise production.

As an example of the diagnostic capabilities of LAFPAs, they were used in a recent study of Mach wave radiation over the range of jet Mach numbers and temperatures shown in Table 1 [73]. Figure 10

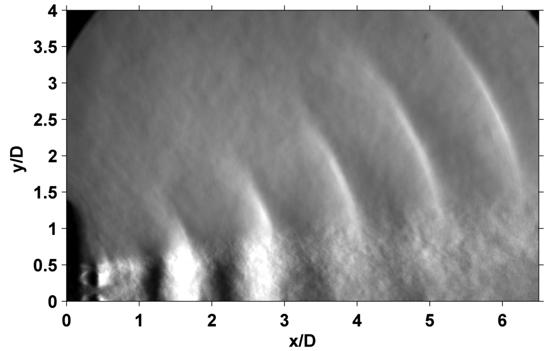

a) $M_j = 1.3$, $TTR = 1.75$

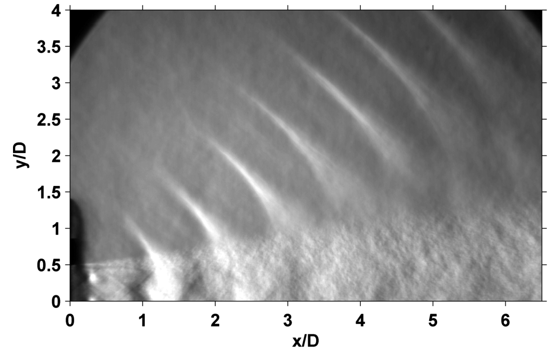

b) $M_j = 1.65$, $TTR = 2.5$

Fig. 10 Phase-averaged schlieren images of Mach 1.3 and 1.65 jets of different temperatures excited with $m = 0$ and $\mathrm{St}_{DF} = 0.6$.

shows two phase-averaged schlieren images of the Mach 1.3 jet with TTR $= 1.75$ ($M_a = 1.49$) and a Mach 1.65 jet with TTR $= 2.5$ ($M_a = 2.1$), both excited with $m = 0$ and $\mathrm{St}_{DF} = 0.6$. The main observations from these images are as follows:

1) Compression waves in the irrotational field coalesce to form the Mach waves.

2) Mach waves are curved at lower M_a and become flat at higher M_a.

3) The radiation angle also changes with M_a.

While the last observation is known in the literature, the other observations (the nature of formation and the change in the Mach wavefront shape) are made possible by the excitation.

V. Conclusions

In this paper, a brief overview of the development of a class of plasma actuators called LAFPAs and their application in high-speed and high-Reynolds-number flow control was provided. Over the past several years, LAFPAs have been used successfully to excite various instabilities in high subsonic and supersonic jets with a focus on either mixing enhancement or noise reduction. Normally, eight of these high-bandwidth (0–200 kHz) actuators are distributed just upstream of the exit of the nozzle, close to the optimal receptivity location of the jet shear layer. With individual control of the actuators, jet shear layer instability, jet column instability, and various jet azimuthal instabilities ($m = 0, 1, 2, 3, \pm 1, \pm 2,$, and ± 4) are excited. The primary control mechanism is localized joule heating, which results in the generation of compression waves.

A brief summary of the work using LAFPAs for jet control is provided, and the capabilities and potential of the actuators and the control technique are highlighted for not only mixing enhancement and noise mitigation but also flow and acoustic diagnostics. The results show that the jet, when operated over a large range of jet Mach numbers (0.9 to 1.65), stagnation temperature ratios (up to 2.5), and Reynolds numbers (0.2×10^6 to 1.65×10^6), responds to the control over a large range of forcing Strouhal numbers and azimuthal modes. Over this range of jet variables, there is a considerable change in the jet acoustic Mach number (0.83 to 2.1) and the convective Mach number (theoretical: 0.43 to 0.92, and empirical: 0.50 to 2.56), a measure of the compressibility level. Yet, the jet response, in terms of generating organized flow structures and their patterns, is similar. The results clearly demonstrate that the jet flowfield and acoustic far field can be dramatically altered, providing a powerful control tool in these practical high-speed and high-Reynolds-number jets. Sample flow results (conditionally averaged Galilean streamlines and Q criterion) and acoustic results (Mach wave radiation) are presented to demonstrate the capabilities of these actuators and the control technique for flow and acoustic diagnostics.

Acknowledgments

The support of this research by the NASA John H. Glenn Research Center at Lewis Field with James Bridges and Cliff Brown and by the U.S. Naval Air Systems Command with John Spyropoulos is greatly appreciated. The help and support of Igor Adamovich and discussions with Datta Gaitonde have been instrumental.

References

[1] Samimy, M., Debiasi, M., Caraballo, E., Serrani, A., Yuan, X., Little, J., and Myatt, J. H., "Feedback Control of Subsonic Cavity Flows Using Reduced-Order Models," *Journal of Fluid Mechanics*, Vol. 579, 2007, pp. 315–346.
doi:10.1017/S0022112007005204

[2] Sinha, A., Kim, K., Kim, J., Serrani, A., and Samimy, M., "Extremizing Feedback Control of a High-Speed and High Reynolds Number Jet," *AIAA Journal*, Vol. 48, No. 2, 2010, pp. 387–399.
doi:10.2514/1.44012

[3] Melton, L. P., Schaeffler, N. W., Yao, C.-S., and Seifert, A., "Active Control of Flow Separation from Supercritical Airfoil Leading-Edge Flap Shoulder," *Journal of Aircraft*, Vol. 42, No. 5, 2005, pp. 1142–1149.
doi:10.2514/1.10294

[4] Little, J., and Samimy, M., "High-Lift Airfoil Separation with Dielectric Barrier Discharge Plasma Actuation," *AIAA Journal*, Vol. 48, No. 12, 2010, pp. 2884–2898.
doi:10.2514/1.J050452

[5] Alkislar, M. B., "Flow Characteristics of a Jet Controlled with Chevron-Microjet Combination for Noise Reduction," AIAA Paper 2009-0851, 2009.

[6] Samimy, M., Kim, J. H., Kastner, J., Adamovich, I., and Utkin, Y., "Active Control of High-Speed and High-Reynolds-Number Jets Using Plasma Actuators," *Journal of Fluid Mechanics*, Vol. 578, No. 1, 2007, pp. 305–330.
doi:10.1017/S0022112007004867

[7] Moreau, E., "Airflow Control by Non-Thermal Plasma Actuators," *Journal of Physics D: Applied Physics*, Vol. 40, No. 3, 2007, pp. 605–636.
doi:10.1088/0022-3727/40/3/S01

[8] Little, J., Takashima, K., Nishihara, M., Adamovich, I., and Samimy, M., "High Lift Airfoil Leading Edge Separation Control with Nanosecond Pulse Driven DBD Plasma Actuators," AIAA Paper 2010-4256, 2010.

[9] Rethmel, C., Little, J., Takashima, K., Sinha, A., Adamovich, I., and Samimy, M., "Flow Separation Control over an Airfoil with Nanosecond Pulse Driven DBD Plasma Actuators," AIAA Paper 2011-0487, 2011.

[10] Samimy, M., Kim, J.-H., Kearney-Fischer, M., and Sinha, A., "Acoustic and Flow Fields of an Excited High Reynolds Number Axisymmetric Supersonic Jet," *Journal of Fluid Mechanics*, Vol. 656, 2010, pp. 507–529.
doi:10.1017/S0022112010001357

[11] Michalke, A., and Fuchs, H. V., "On Turbulence and Noise of an Axisymmetric Shear Flow," *Journal of Fluid Mechanics*, Vol. 70, No. 1, 1975, pp. 179–205.
doi:10.1017/S0022112075001966

[12] Zaman, K. B. M. Q., and Hussain, A. K. M. F., "Turbulence Suppression in Free Shear Flows by Controlled Excitation," *Journal of Fluid Mechanics*, Vol. 103, 1981, pp. 133–159.
doi:10.1017/S0022112081001274

[13] Crow, S. C., and Champagne, F. H., "Orderly Structure in Jet Turbulences," *Journal of Fluid Mechanics*, Vol. 48, No. 3, 1971, pp. 547–591.

doi:10.1017/S0022112071001745

[14] Michalke, A., and Hermann, G., "ON THE Inviscid Instability of a Circular Jet with External Flow," *Journal of Fluid Mechanics*, Vol. 114, 1982, pp. 343–359. doi:10.1017/S0022112082000196

[15] Cohen, J., and Wygnanski, I., "The Evolution of Instabilities in the Axisymmetric Jet. Part 1, The Linear Growth of Disturbances Near Nozzle," *Journal of Fluid Mechanics*, Vol. 176, 1987, pp. 191–219. doi:10.1017/S0022112087000624

[16] Barone, M. F., and Lele, S. K., "Receptivity of the Compressible Mixing Layer," *Journal of Fluid Mechanics*, Vol. 540, 2005, pp. 301–335. doi:10.1017/S0022112005005884

[17] Brown, G. L., and Roshko, A., "On Density Effects and Large Structure in Turbulent Mixing Layers," *Journal of Fluid Mechanics*, Vol. 64, No. 4, 1974, pp. 775–816. doi:10.1017/S002211207400190X

[18] Moore, C. J., "The Role of Shear-Layer Instability Waves in Jet Exhaust Noise," *Journal of Fluid Mechanics*, Vol. 80, No. 2, 1977, pp. 321–367. doi:10.1017/S0022112077001700

[19] Deneuville, P. N., and Jacques, J. R., "Jet Noise Amplification: A Practically Important Problem," AIAA Paper 1977-1368, 1977.

[20] Lu, H. Y., "Effect of Excitation on Coaxial Jet Noise," *AIAA Journal*, Vol. 21, No. 2, 1983, pp. 214–220. doi:10.2514/3.8056

[21] Tanna, H. K., and Ahuja, K. K., "Tone Excited Jets. I: Introduction," *Journal of Sound and Vibration*, Vol. 102, No. 1, 1985, pp. 57–61. doi:10.1016/S0022-460X(85)80102-4

[22] Moore, C. J., "The Effect of Shear Layer Instability on Jet Exhaust Noise," *Structure and Mechanisms of Turbulence II*, Vol. 76, 1977, pp. 254–264.doi:10.1007/BFb0012628

[23] Crighton, D. G., "Jet Noise and the Effects of Jet Forcing," *Lecture Notes in Physics*, Vol. 136, 1981, pp. 340–362. doi:10.1007/3-540-10289-2_34

[24] Bechert, D. W., and Pfizenmaier, E., "On The Amplification of Broad Band Jet Noise by a Pure Tone Excitation," *Journal of Sound and Vibration*, Vol. 43, No. 3, 1975, pp. 581–587. doi:10.1016/0022-460X(75)90015-2

[25] Hussain, A. K. M. F., and Zaman, K. B. M. Q., "The 'Preferred Mode' of the Axisymmetric Jet," *Journal of Fluid Mechanics*, Vol. 110, 1981, pp. 39–71. doi:10.1017/S0022112081000608

[26] Ahuja, K. K., and Blakney, D. F., "Tone Excited Jets, Part IV: Acoustic Measurements," *Journal of Sound and Vibration*, Vol. 102, No. 1, 1985, pp. 93–117. doi:10.1016/S0022-460X(85)80105-X

[27] Kibens, V., "Discrete Noise Spectrum Generated by an Acoustically Excited Jet," *AIAA Journal*, Vol. 18, No. 4, 1980, pp. 434–441. doi:10.2514/3.50776

[28] Hussain, A. K. M. F., and Hasan, M. A. Z., "Turbulence Suppression in Free Turbulent Shear Flows Under Controlled Excitation, Part 2. Jet-Noise Reduction," *Journal of Fluid Mechanics*, Vol. 150, 1985, pp. 159–168. doi:10.1017/S0022112085000076

[29] Jubelin, B., "New Experimental Studies on Jet Noise Amplification," AIAA Paper 1980-0961, 1980.

[30] Heavens, S. N., "Visualization of the Acoustic Excitation of a Subsonic Jet," *Journal of Fluid Mechanics*, Vol. 100, No. 1, 1980, pp. 185–192. doi:10.1017/S0022112080001073

[31] Zaman, K. B. M. Q., and Hussain, A. K. M. F., "Vortex Pairing in a Circular Jet Under Controlled Excitation, Part 1. General Jet Response," *Journal of Fluid Mechanics*, Vol. 101, No. 3, 1980, pp. 449–491. doi:10.1017/S0022112080001760

[32] Ahuja, K. K., and Whiffen, M. C., "Tone Excited Jets. II: Flow Visualization," *Journal of Sound and Vibration*, Vol. 102, No. 1, 1985, pp. 63–69. doi:10.1016/S0022-460X(85)80103-6

[33] Kusek, S. M., Corke, T. C., and Reisenthel, P., "Seeding of Helical Modes in the Initial Region of an Axisymmetric Jet," *Experiments in Fluids*, Vol. 10, Nos. 2–3, 1990, pp. 116–124. doi:10.1007/BF00215019

[34] Corke, T. C., and Kusek, S. M., "Resonance in Axisymmetric Jets with Controlled Helical-Mode Input," *Journal of Fluid Mechanics*, Vol. 249, 1993, pp. 307–336. doi:10.1017/S0022112093001193

[35] Adelgren, R. G., Elliott, G. S., Crawford, J. B., Carter, C. D., Donbar, J. M., and Grosjean, D. F., "Axisymmetric Jet Shear-Layer Excitation by Laser Energy and Electric Arc Discharges," *AIAA Journal*, Vol. 43, No. 4, 2005, pp. 776–791. doi:10.2514/1.8548

[36] Hussain, A. K. M. F., "Coherent Structures and Turbulence," *Journal of Fluid Mechanics*, Vol. 173, 1986, pp. 303–356. doi:10.1017/S0022112086001192

[37] Chan, Y. Y., "Spatial Waves in Turbulent Jets," *Physics of Fluids*, Vol. 17, No. 1, 1974, pp. 46–53. doi:10.1063/1.1694612

[38] Morrison, G. L., and McLaughlin, D. K., "Instability Process in Low Reynolds Number Supersonic Jets," *AIAA Journal*, Vol. 18, No. 7, 1980, pp. 793–800. doi:10.2514/3.7688

[39] Cohen, J., and Wygnanski, I., "The Evolution of Instabilities in the Axisymmetric Jet, Part 2: The Flow Resulting from the Interaction Between Two Waves," *Journal of Fluid Mechanics*, Vol. 176, 1987, pp. 221–235. doi:10.1017/S0022112087000636

[40] Morrison, G. L., and McLaughlin, D. K., "Noise Generation by Instabilities in Low Reynolds Number Supersonic Jets," *Journal of Sound and Vibration*, Vol. 65, No. 2, 1979, pp. 177–191. doi:10.1016/0022-460X(79)90512-1

[41] Bridges, J., and Hussain, F., "Direct Evaluation of Aeroacoustic Theory in a Jet," *Journal of Fluid Mechanics*, Vol. 240, 1992, pp. 469–501. doi:10.1017/S0022112092000168

[42] Lepicovsky, J., Ahuja, K. K., and Salikuddin, M., "An Experimental Study of Tone-Excited Heated Jets," *Journal of Propulsion and Power*, Vol. 2, No. 2, 1986, pp. 149–154. doi:10.2514/3.22859

[43] Kibens, V., Dorris, J., III, Smith, D. M., and Mossman, M. F., "Active Flow Control Technology Transition: The Boeing ACE Program," AIAA Paper 1999-3507, 1999.

[44] Ahuja, K. K., Lepicovsky, J., and Burrin, R. H., "Noise and Flow Structure of a Tone-Excited Jet," *AIAA Journal*, Vol. 20, No. 12, 1982, pp. 1700–1706. doi:10.2514/3.8007

[45] Lepicovsky, J., and Brown, W. H., "Effects Of Nozzle Exit Boundary-Layer Conditions on Excitability Of Heated Free Jets," *AIAA Journal*, Vol. 27, No. 6, 1989, pp. 712–718. doi:10.2514/3.10170

[46] Low, K., Hadidi, B. E., Andino, M., Berdanier, R., and Glauser, M., "Investigation of Different Active Flow Control Strategies for High Speed Jets Using Synthetic Jet Actuators," AIAA Paper 2010-4267, 2010.

[47] Utkin, Y. G., Keshav, S., Kim, J.-H., Kastner, J., Adamovich, I. V., and Samimy, M., "Development and Use of Localized Arc Filament Plasma Actuators for High-Speed Flow Control," *Journal of Physics D: Applied Physics*, Vol. 40, No. 3, 2007, pp. 685–694. doi:10.1088/0022-3727/40/3/S06

[48] Samimy, M., Adamovich, I., Webb, B., Kastner, J., Hileman, J., Keshav, S., and Palm, P., "Development and Characterization of Plasma Actuators for High-Speed Jet Control," *Experiments in Fluids*, Vol. 37, No. 4, 2004, pp. 577–588. doi:10.1007/s00348-004-0854-7

[49] Hahn, C., Kearney-Fischer, M., and Samimy, M., "Effects of Ring Groove and Duty Cycle on Plasma Actuator Performance in High Speed Jets," *Experiments in Fluids* [online], Aug. 2011. doi:10.1007/s00348-011-1172-5

[50] Kleinman, R. R., Bodony, D. J., and Freund, J. B., "Shear-Flow Excitation Mechanisms of Recessed Localized Arc-Filament Plasma Actuators," *Physics of Fluids*, Vol. 22, 2010, Paper 116103. doi:10.1063/1.3507317

[51] Kim, J., Nishihara, M., Adamovich, I., Samimy, M., Gorbatov, S. V., and Pliavaka, F. V., "Development of Localized Arc Filament RF Plasma Actuators for High-Speed and High Reynolds Number Flow Control," *Experiments in Fluids*, Vol. 49, 2010, pp. 497–511. doi:10.1007/s00348-010-0819-y

[52] Gaitonde, D., "Simulation of Supersonic Nozzle Flows with Plasma-Based Control," AIAA Paper 2009-4187, 2009.

[53] Gaitonde, D. V., and Samimy, M., "Coherent Structures in Plasma-Actuator Supersonic Jets: Axisymmetric and Mixed Azimuthal Modes," *Physics of Fluids*, Vol. 23, 2011, Paper 095104. doi:10.1063/1.3627215

[54] Kim, J., Afshari, A., Bodony, D. J., and Freund, J. B., "LES Investigation of a Mach 1.3 Jet with and Without Plasma Actuators," AIAA Paper 2009-0290, 2009.

[55] Kearney-Fischer, M., Kim, J.-H., and Samimy, M., "Control of a High Reynolds Number Mach 0.9 Heated Jet Using Plasma Actuators," *Physics of Fluids*, Vol. 21, 2009, pp. 095101. doi:10.1063/1.3210771

[56] Kearney-Fischer, M., Kim, J.-H., and Samimy, M., "Flow Control of a High Reynolds Number Mach 1.3 Heated Jet Using Plasma Actuators,"

AIAA Paper 2010-4418, 2010.
[57] Samimy, M., Kim, J. H., Kastner, J., Adamovich, I., and Utkin, Y., "Active Control of a Mach 0.9 Jet for Noise Mitigation Using Plasma Actuators," *AIAA Journal*, Vol. 45, No. 4, 2007, pp. 890–901. doi:10.2514/1.27499
[58] Kim, J. H., Kastner, J., and Samimy, M., "Active Control of a High Reynolds Number Mach 0.9 Axisymmetric Jet," *AIAA Journal*, Vol. 47, No. 1, 2009, pp. 116–128. doi:10.2514/1.36801
[59] Kim, J.-H., and Samimy, M., "Effects of Active Control on the Flow Structure in a High Reynolds Number Supersonic Jet," *International Journal of Flow Control*, Vol. 1, No. 2, 2009, pp. 99–117. doi:10.1260/175682509788913344
[60] Kastner, J., Kim, J.-H., and Samimy, M., "A Study of the Correlation of Large-Scale Structure Dynamics and Far-Field Radiated Noise in an Excited Mach 0.9 Jet," *International Journal of Aeroacoustics*, Vol. 8, No. 3, 2009, pp. 231–259. doi:10.1260/147547208786940008
[61] Kearney-Fischer, M., Kim, J.-H., and Samimy, M., "Noise Control of a High Reynolds Number High Speed Heated Jet Using Plasma Actuators," *International Journal of Aeroacoustics*, Vol. 10, Nos. 5–6, 2011, pp. 635–658. doi:10.1260/1475-472X.10.5-6.635
[62] Kim, J.-H., Kearney-Fischer, M., Samimy, M., and Gogineni, S., "Far-Field Noise Control in Supersonic Jets Using Conical and Contoured Nozzles," *Journal of Engineering for Gas Turbines and Power*, Vol. 133, Aug. 2011, Paper 081201. doi:10.1115/1.4002811
[63] Sinha, A., Serrani, A., and Samimy, M., "Initial Development of Reduced-Order Models for Feedback Control of Axisymmetric Jets," *International Journal of Flow Control*, Vol. 2, No. 1, 2010, pp. 39–60. doi:10.1260/1756-8250.2.1.39
[64] Bechert, D. W., and Stahl, B., "Excitation of Instability Waves in Free Shear Layers, Part 2. Experiments," *Journal of Fluid Mechanics*, Vol. 186, 1988, pp. 63–84. doi:10.1017/S0022112088000047
[65] Thurow, B. S., Jiang, N., Kim, J.-H., Lempert, W., and Samimy, M., "Issues with Measurements of the Convective Velocity of Large-Scale Structures in the Compressible Shear Layer of a Free Jet," *Physics of Fluids*, Vol. 20, No. 6, 2008, Paper 066101. doi:10.1063/1.2926757.
[66] Petitjean, B. P., McLaughlin, D. K., and Morris, P. J., "An Experimental Investigation of Density Gradient Fluctuations in High-Speed Jets Using Optical Deflectometry," AIAA Paper 2006-2533, 2006.
[67] Lau, J. C., "Laser Velocimeter Correlation Measurements in Subsonic and Supesonic Jets," *Journal of Sound and Vibration*, Vol. 70, No. 1, 1980, pp. 85–101. doi:10.1016/0022-460X(80)90556-8
[68] Doty, M. J., and McLaughlin, D. K., "Space-Time Correlation Measurements of High-Speed Axisymmetric Jets Using Optical Deflectometry," *Experiments in Fluids*, Vol. 38, No. 4, 2005, pp. 415–425. doi:10.1007/s00348-004-0920-1
[69] Hunt, J. C. R., Wray, A. A., and Moin, P., "Eddies, Stream, and Convergence Zones in Turbulent Flows," Center for Turbulence Research Rept. CTR-S88, Stanford, CA, 1988, p. 193.
[70] Jeong, J., and Hussain, F., "On the Identification of a Vortex," *Journal of Fluid Mechanics*, Vol. 285, 1995, pp. 69–94. doi:10.1017/S0022112095000462
[71] Zhou, J., Adrian, R. J., Balachandar, S., and Kendall, T. M., "Mechanisms for Generating Coherent Packets of Hairpin Vortices In Channel Flow," *Journal of Fluid Mechanics*, Vol. 387, 1999, pp. 353–396. doi:10.1017/S002211209900467X
[72] Adrian, R. J., Christensen, K. T., and Liu, Z.-C., "Analysis and Interpretation of Instantaneous Turbulent Velocity Fields," *Experiments in Fluids*, Vol. 29, 2000, pp. 275–290. doi:10.1007/s003489900087
[73] Kearney-Fischer, M., Kim, J.-H., and Samimy, M., "A Study of Mach Wave Radiation Using Active Control," *Journal of Fluid Mechanics*, Vol. 681, Aug. 2011, pp. 261–292. doi:10.1017/jfm.2011.196
[74] Samimy, M., Kastner, J., Kim, J. H., Utkin, Y., Adamovich, I., and Brown, C., "Flow and Noise Control in High Speed and High Reynolds Number Jets Using Plasma Actuators," AIAA Paper 2846, 2006.
[75] George, W. K., Beuther, P. D., and Arndt, R. E. A., "Pressure Spectra in Turbulent Free Shear Flows," *Journal of Fluid Mechanics*, Vol. 148, 1984, pp. 155–191. doi:10.1017/S0022112084002299
[76] Arndt, R. E. A., Long, D. F., and Glauser, M. N., "The Proper Orthogonal Decomposition of Pressure Fluctuations Surrounding a Turbulent Jet," *Journal of Fluid Mechanics*, Vol. 340, 1997, pp. 1–33. doi:10.1017/S0022112097005089
[77] Tinney, C. E., Ukeiley, L. S., and Glauser, M. N., "Low-Dimensional Characteristics of a Transonic Jet, Part 2. Estimate and Far-Field Prediction," *Journal of Fluid Mechanics*, Vol. 615, 2008, pp. 53–92. doi:10.1017/S0022112008003601
[78] Suzuki, T., and Colonius, T., "Instability Waves in a Subsonic Round Jet Detected Using a Near-Field Phased Microphone Array," *Journal of Fluid Mechanics*, Vol. 565, 2006, pp. 197–226. doi:10.1017/S0022112006001613
[79] Hall, J. W., Pinier, J., Hall, A. e., and Glauser, M., "Two-Point Correlations of the Near and Far-Field Pressure in a Transonic Jet," American Soc. of Mechanical Engineers Paper FEDSM2006-98458, Fairfield, NJ , 2006.
[80] Jordan, P., and Gervais, Y., "Subsonic Jet Aeroacoustics: Associating Experiment, Modelling and Simulation," *Experiments in Fluids*, Vol. 44, No. 1, 2008, pp. 1–21. doi:10.1007/s00348-007-0395-y
[81] Sinha, A., Serrani, A., and Samimy, M., "Development of Empirical Estimators for Feedback Control of Axisymmetric Jets," *AIAA Journal*, Vol. 49, No. 9, 2011, pp. 1971–1987. doi:10.2514/1.J050966

L. Maurice
Associate Editor